Electronic Supplementary Material (ESI) for Nanoscale.

Supporting Information

Crystal engineering of zeolites with graphene

Paul Gebhardt[a†], Sebastian W. Pattinson[b†], Zhibin Ren[b], James A. Elliott[b], David J. Cooke[d], Dominik Eder[a]*

TG/DTA results

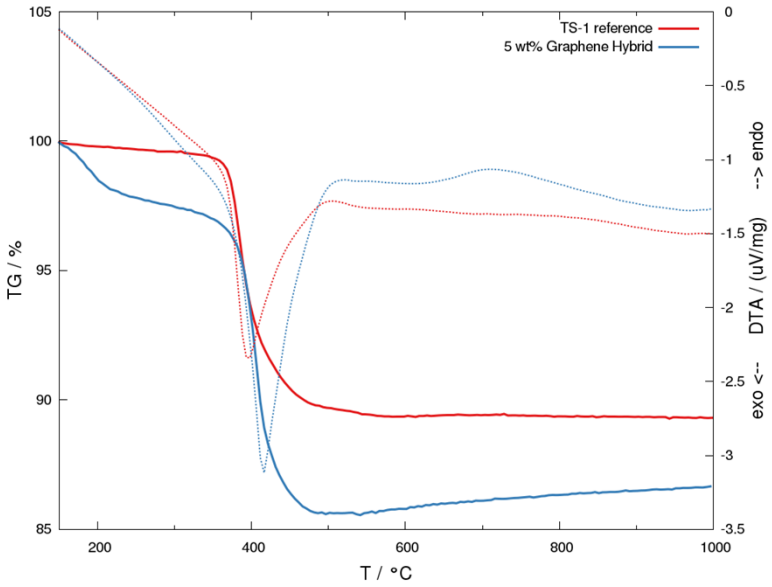

Fig. S1: STA plot for TS-1 reference sample (red) and 5 wt% graphene hybrid (blue).

The TG plot for pure TS-1 show a sharp weight loss starting at 380 °C combined with an exothermic peak in the respective DTA curve. This indicates the oxidative removal of the micropore template (TPAOH). The respective peak for the 5 wt% graphene hybrid is shifted to 400 °C. This may indicate the blocking of micropores through adsorption of graphene, thus restricting the removal of TPAOH from the micropores. The early weight loss in this sample can be assigned to BA (bp.: 205 °C). Furthermore the DTA plot shows exothermic peaks at temperatures above 500 °C that are associated to the oxidation of graphene.

BET/BJH results

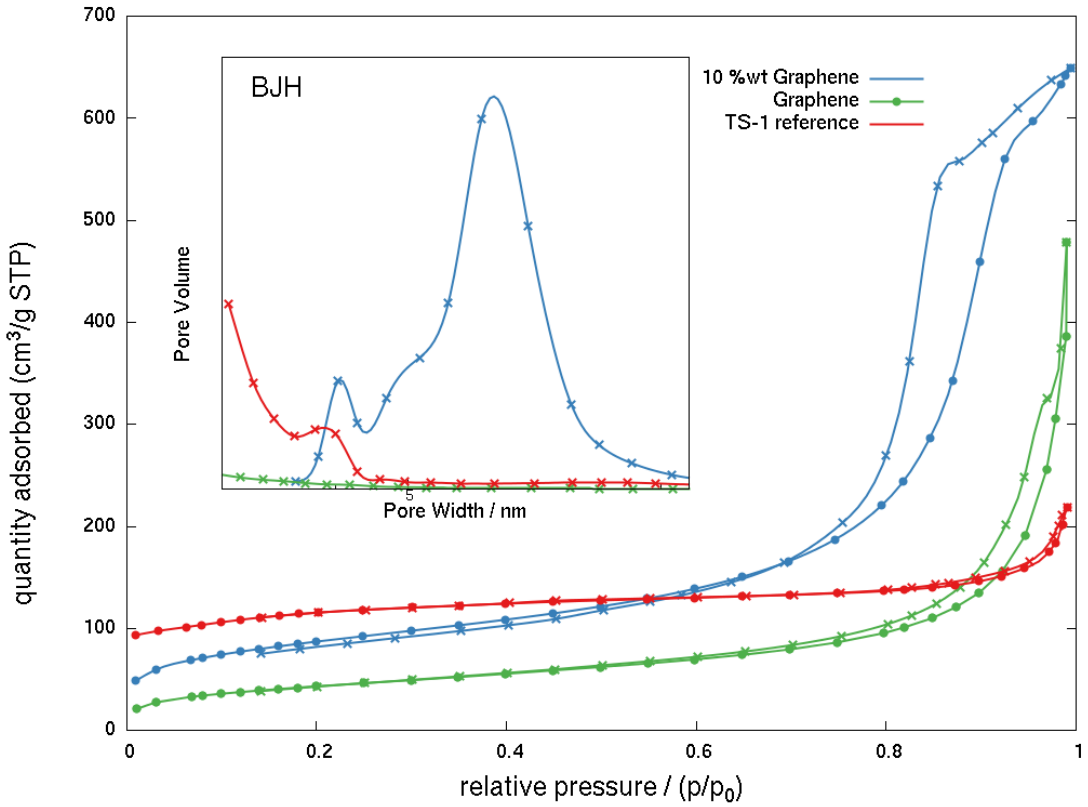

Figure S2: Physisorption isotherms of TS-1, Graphene and 10 wt% HG hybrid. Inset: BJH desorption pore size distribution.

Figure S2 shows typical isotherms of N_2-physisorption for the individual components HG-graphene and TS-1 as well as a 10 wt% hybrid of TS-1 with HG-graphene.
The most intriguing feature is the distinct mesoporosity in the hybrid. The pore size distribution in the inset following the BJH theorem reveals the presence of large mesopores (8-9 nm).

FTIR spectroscopy

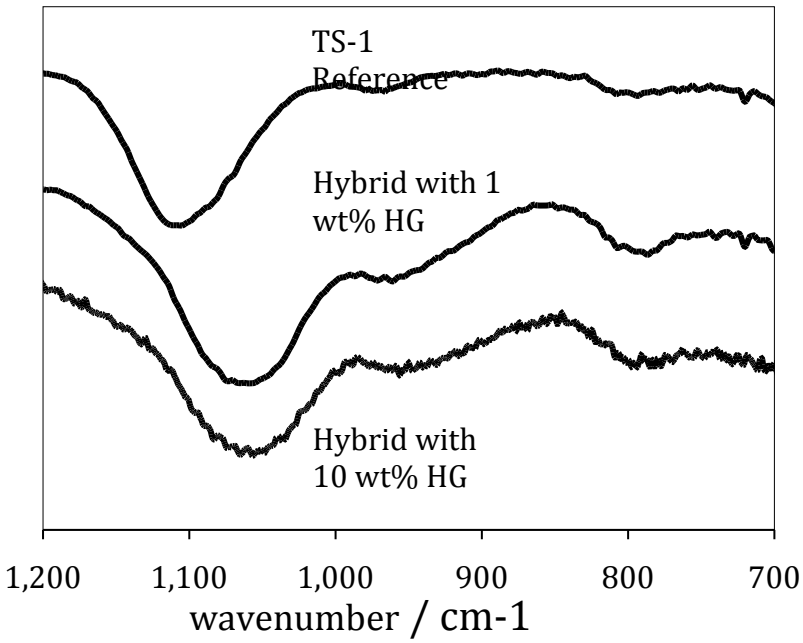

Fig. S3 FTIR spectra of TS-1 reference and TS-1 HG hybrids with 1 and 10 wt%.

Figure S3 shows FTIR spectra for the TS-1 reference and two hybrids (i.e. with 1 and 10 wt% HG). The band around 1050-1100 cm^{-1} in the hybrids is considerably shifted to lower wavenumbers compared to the reference, which is attributed to an interaction between the TS-1 surface and adsorbed graphene.

UV-VIS spectroscopy

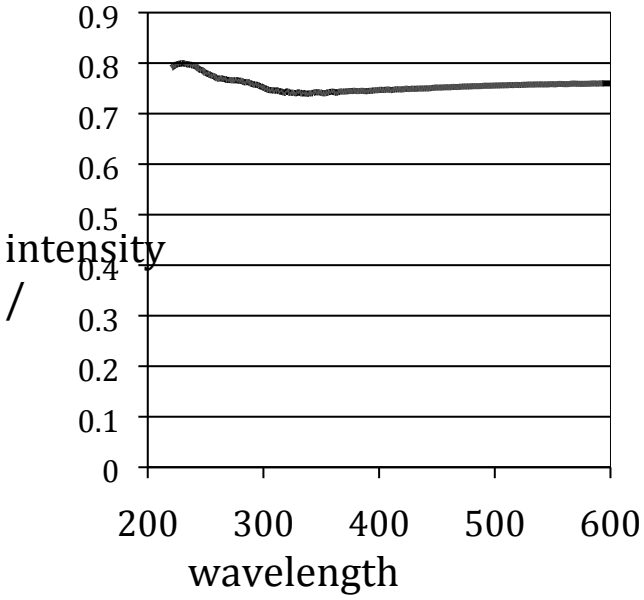

Fig. S4: UV-vis spectrum of 10 wt% TS-1 HG hybrid.

Figure S4 shows a typical UV-vis spectrum of the TS-1 hybrid with 10 wt% HG including the characteristic absorption for tetrahedrally coordinated Ti (around 220 cm^{-1}). The shoulder at 270 cm^{-1} and the further increase of absorption at higher wave length is attributed to graphene.

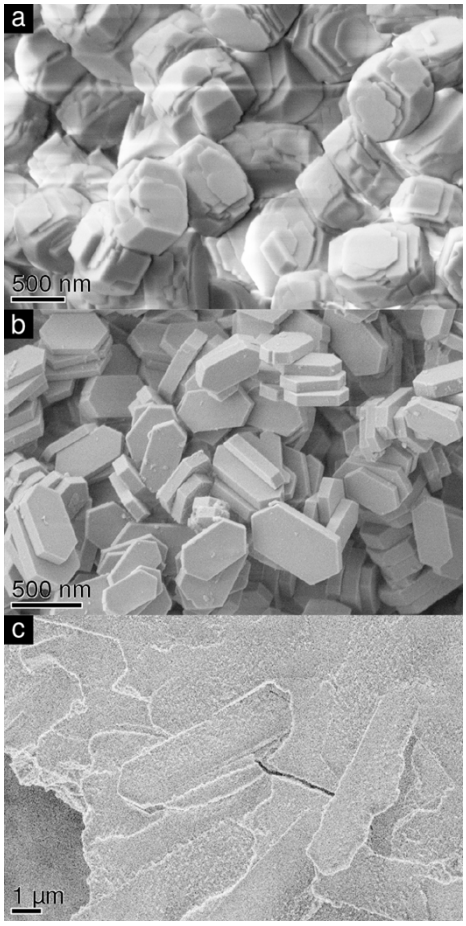

Fig. S5: SEM micrographs of pure TS-1 (without graphene) synthesized from diluted zeolite sol; (a) 1x, (b) 5x, (c) 10x

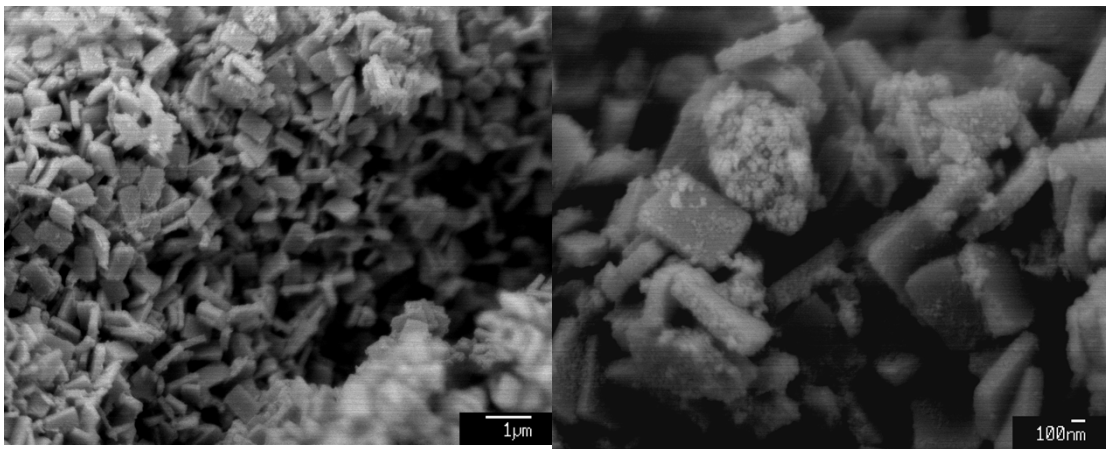

Fig S6: SEM micrographs of 5 wt% TS-1 HG hybrids.

Estimation of the maximum stable size of TS-1 nanocrystal with bound graphene due to lattice strain.

Consider a simple model for TS-1 nanocrystal, shown in Fig. S7, which is comprised of a block of lateral dimensions *a* by *a* and thickness *c*. The nanocrystal orientation is such that the *a*-*a* surface is (010), and the *a*-c surface is (001), with respective surface energies for native TS-1 and TS-1 with bound graphene shown in Table 2.

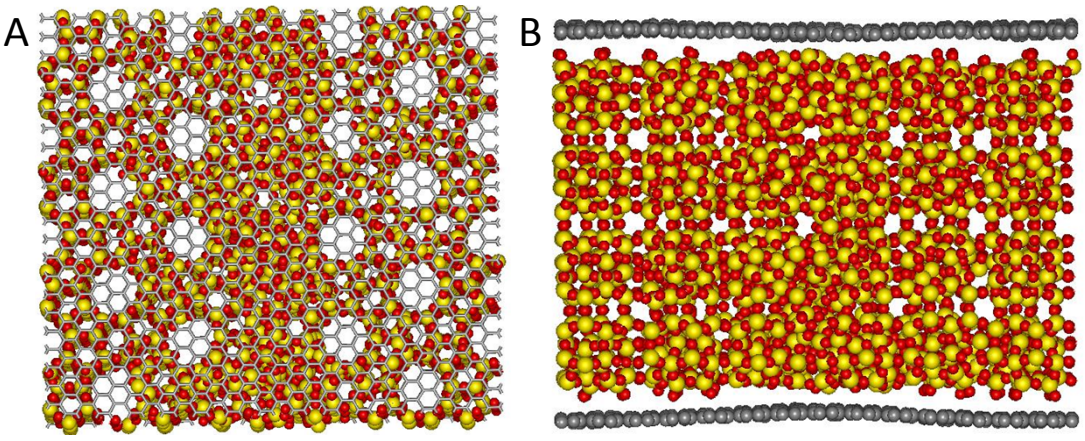

Fig. S7: Direct interaction of graphene with TS-1 (010) surface cell a) top-down b) side view (along [001]). The graphene-TS-1 interaction energies are calculated using methods described in main text of article.

We assume that graphene binds to (010), which is the predominant surface observed experimentally and the second to lowest-ranked surface energy for our calculations of TS-1 with bound graphene. This induces a misfit stress related to the energy difference between (010) for pure TS-1 and TS-1+graphene, multiplied by the area (a^2). If this exceeds the energy required to break the crystal along direction perpendicular to its thickness (parallel to graphene sheet), which is given by $2ac\gamma_{001}$ (because there are two surfaces created on breakage) then the crystal will be unstable. This can then be rearranged to show that the following inequality should be satisfied to avoid breakage:

$$\frac{a}{c} < \frac{2\gamma_{001}}{\gamma_{010} - \gamma_{010}^{g}} \qquad \backslash\text{* MERGEFORMAT (0.1)}$$

where the superscript *g* denotes a surface energy of TS-1 with bound graphene. Inserting the appropriate numbers from Table 2, yields $a/c < 45$, which implies that

TS-1 nanocrystals with bound graphene will be unstable if their width exceeds 45 times their thickness.

Repeating the calculation for a different orientation of TS-1 nanocrystal, with graphene bound to (101), which is lowest-ranked surface energy for our calculations of TS-1 with bound graphene, and fracture surface (010), the no-fracture condition becomes:

$$\frac{a}{c} < \frac{\gamma_{101} - \gamma_{101}^{g}}{2\gamma_{010}} \qquad \text{* MERGEFORMAT (0.2)}$$

which yields $a/c < 0.111$ after substitution of the appropriate surface energies from Table 2, which implies that TS-1 nanocrystals with bound graphene will be unstable if their thickness is less than 9 times their width.

Molecular Modelling of BA – TS-1 Interface

To probe the interface between the benzyl alcohol (BA) solvent and TS-1 we have adopted the approach of our previous study of TiO_2[26] where slab terminated by a particular mineral surface is brought into contact with a box containing liquid BA and the system relaxed using molecular dynamics.

We have focused on three TS-1 surfaces: two that are predicted to dominate the equilibrium morphology, (010) and (101), and one that is absent from the morphology, (001). The adsorption profile was determined by plotting the density of the BA molecules as a function of perpendicular distance from the surface (ρ(z)) and, if it is assumed that the simulation has reached equilibrium, then this profile is a reasonable estimate for the partition function and hence the free energy change associated with molecules approaching the surface can be estimated from the relationship $\Delta A = -RT \ln[\rho(z) - \rho(z_0)]$, where $\rho(z_0)$ is the density of liquid BA. The density profiles are shown in Figures S8, S10 and S12, with corresponding free energy profiles in S9, S11 and S13.

In the case of BA approaching the (001) surface, there is little or no free energy barrier to adsorption (Figure S9), however the adsorption well is itself only shallow (< 1 kJ mol^{-1}) meaning molecules will also be able to easily desorb from the surface leading to a highly mobile interface, which is evident in the density profile (Figure S8)

by the fact that the density only falls to half the value of the bulk solvent between the peak representing the adsorption layer and the bulk solvent.

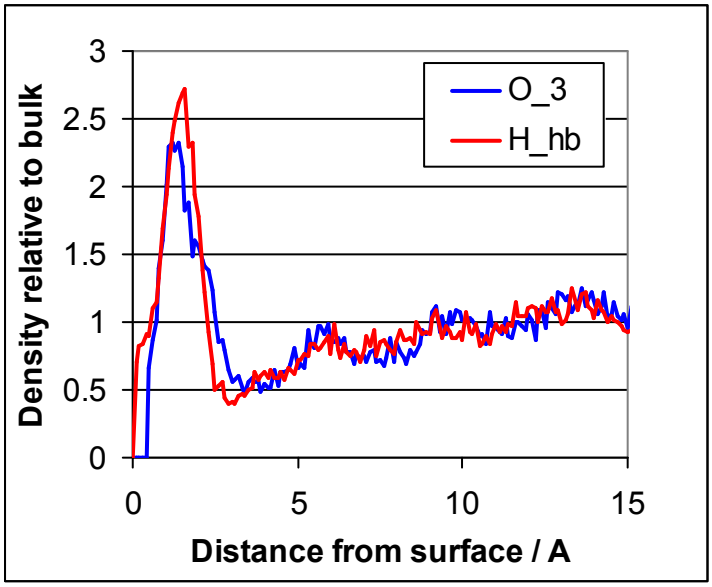

Figure S8 Density of BA perpendicular to the (001) surface of TS-1

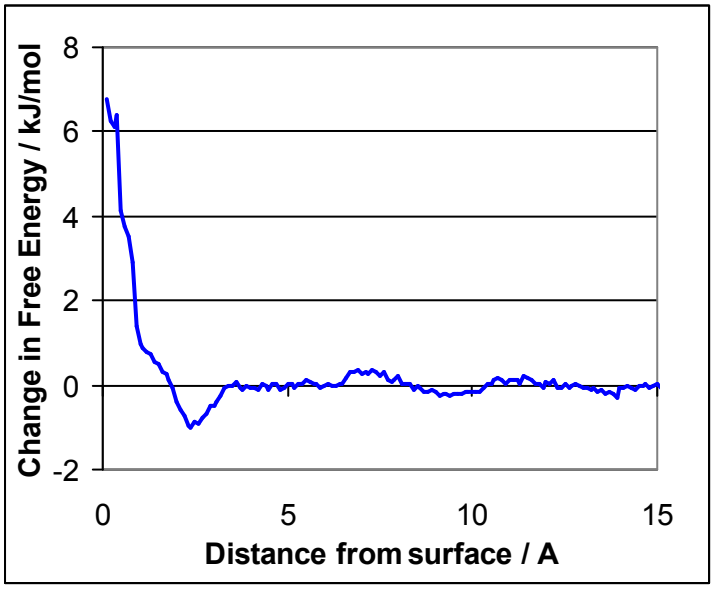

Figure S9 Change in free energy of BA as a function of perpendicular distance from the (001) surface of TS-1

By comparison, inspection of the profiles describing BA approaching the more stable (010) and (101) surfaces reveals a more complex adsorption profile containing several maxima and minima (Figure S10 and Figure S12) and the density falling close to zero between the adsorption layer and the bulk solvent, indicating there is far less movement of molecules in and out of the adsorption layer of these more stable surfaces. When the density profile is transformed into a measure of free energy

(Figures S11 and S13), this leads to an energy profile containing a series of wells and peaks with the adsorption and desorption energy (defined as a molecule moving between the adsorption layer and the second energy minima or vice versa) being roughly equal and calculated to be around 2 kJ mol^{-1}, or close to *RT* under standard conditions. Also noteworthy is the fact that there is a low energy barrier for the molecule to pass from the bulk solvent into the second adsorption layer but the energy barrier for the molecule to desorb back into the bulk solvent is in excess of 1 kJ mol^{-1}.

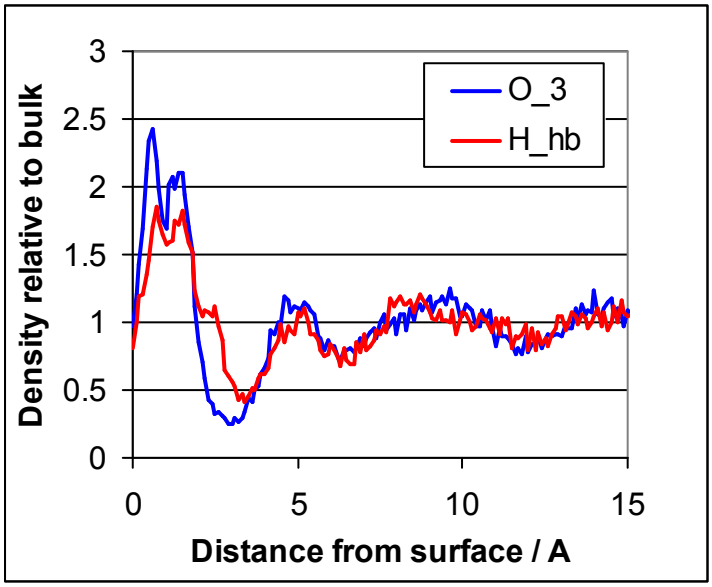

Figure S10 Density of BA perpendicular to the (010) TS-1 surface

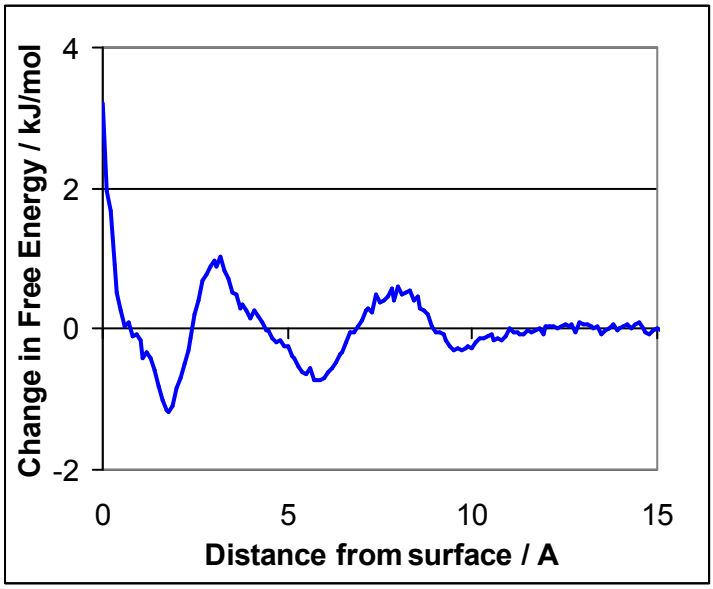

Figure S11 Change in free energy of BA as a function of perpendicular distance from the (010) surface of TS-1

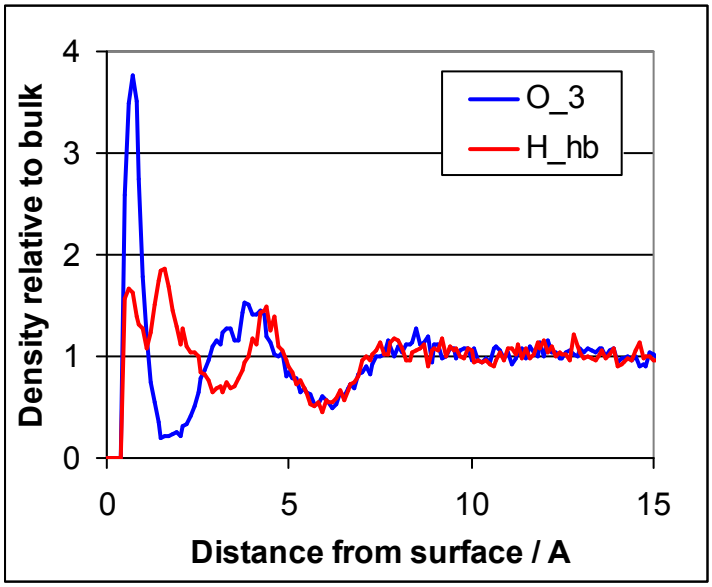

Figure S12 Density of BA perpendicular to the (101) surface of TS-1

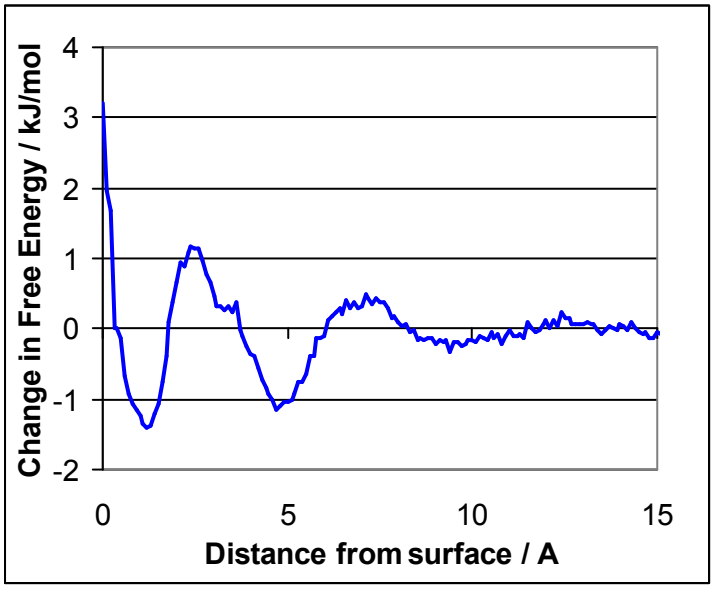

Figure S13 Change in free energy of BA as a function of perpendicular distance from the (101) surface of TS-1

Effect of various process parameters on the shape of TS-1 particles

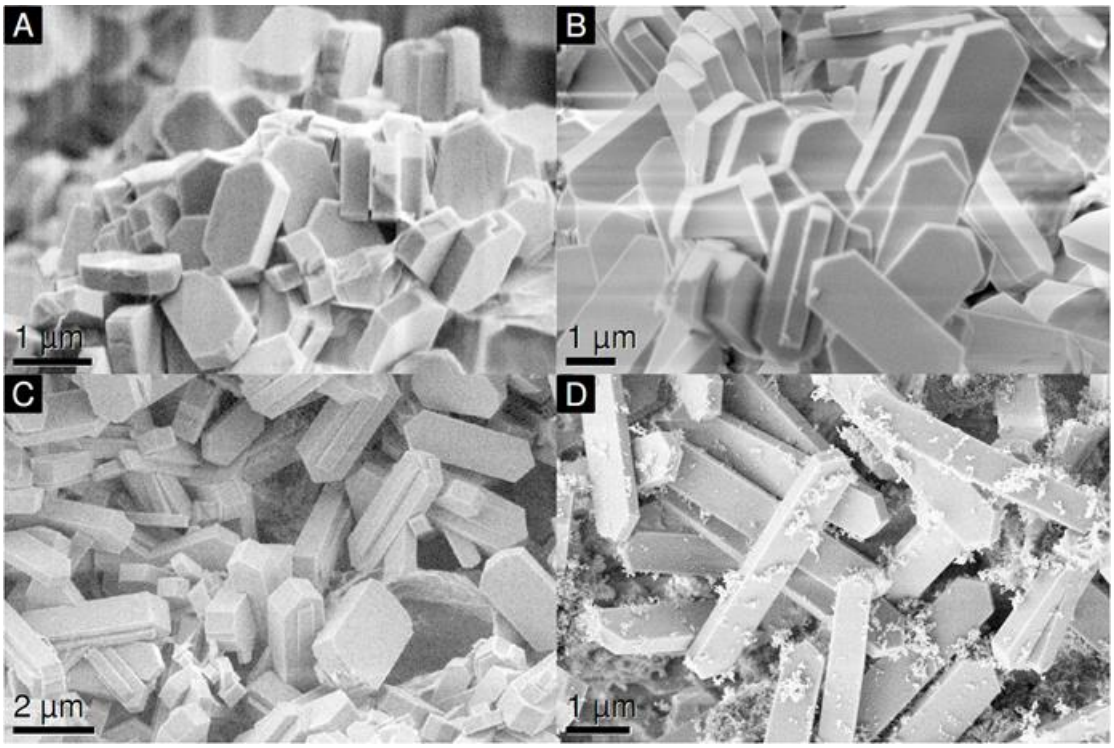

Figure S14: SEM images of TS-1 produced with a) 5 wt%, b) 10 wt%, c) 15 wt%, and d) 20 wt% GO, documenting that GO affects the shape of TS-1 particles in a similar way as RGO.

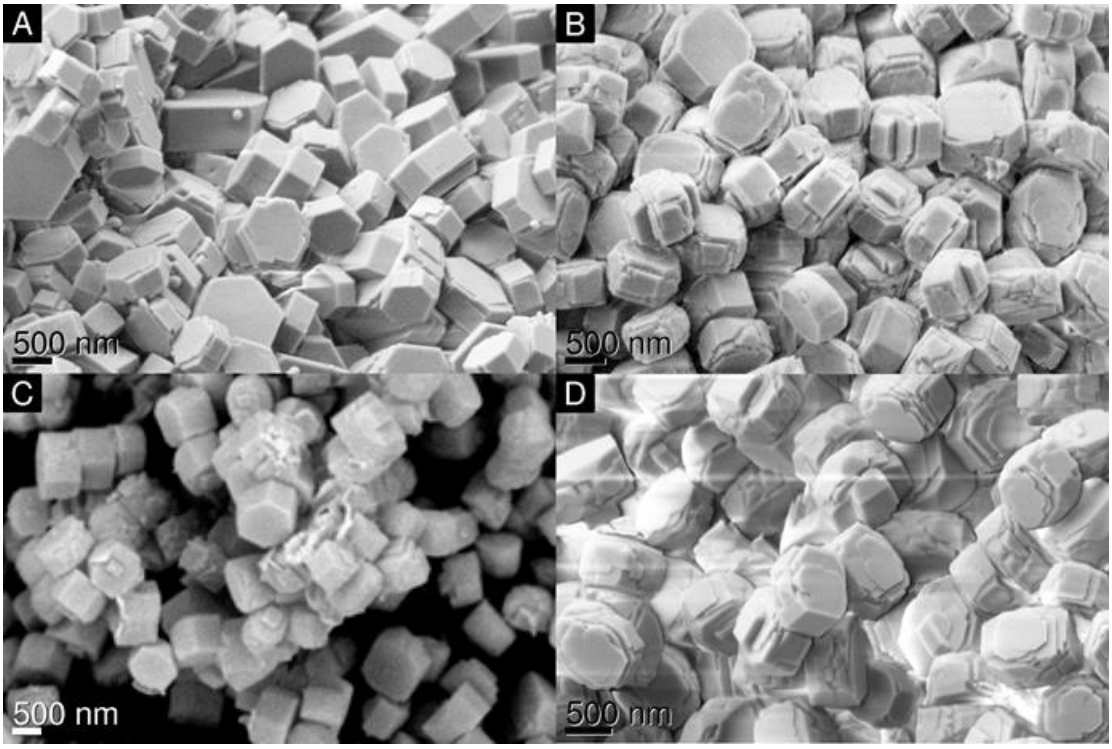

Figure S15: SEM images of TS-1 produced in absence of graphene with various molar ratios of BA with respect to combined Ti and Si precursors of a) 0, b) 0.15, c) 0.3, and d) 0.5. These results confirm that BA had only a negligible effect on the shape of TS-1.

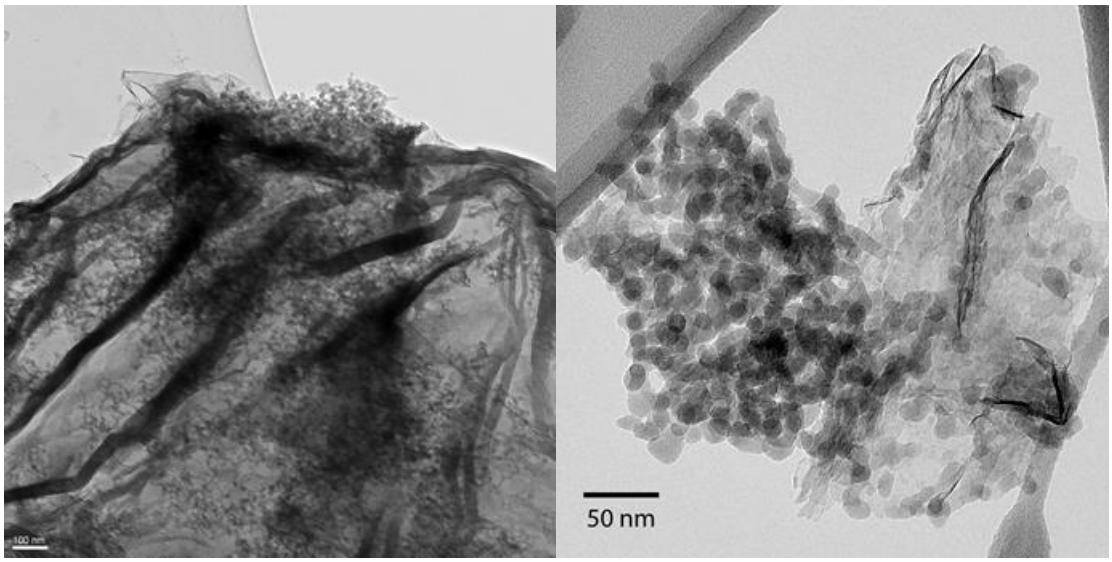

Figure S16: Additional TEM images of TS-1 produced with 10 wt% HG-graphene.